

## Development of analysis strategy for continuous total geomagnetic field data around Mt. Fuji

ABE, Satoshi<sup>1\*</sup> ; MIYAHARA, Basara<sup>1</sup> ; MORISHITA, Hitoshi<sup>1</sup> ; KOBAYASHI, Katsuhiko<sup>1</sup> ; TOYOFUKU, Takashi<sup>1</sup> ; KOYAMA, Takao<sup>2</sup> ; OGAWA, Tsutomu<sup>2</sup>

<sup>1</sup>GSI of Japan, <sup>2</sup>Earthquake Research Institute, The University of Tokyo

Geospatial Information Authority of Japan (GSI) has conducted continuous total geomagnetic field observation at Fuji Yoshida observation station (FUJ), which is located the northeast mountainside of Mt. Fuji, and Fuji-City observation station (FJI), which is located at the southern bottom of Mt. Fuji, since 2000. These stations were established in order to enhance observation infrastructure to monitor low-frequency earthquakes underneath Mt. Fuji which had rapidly increased since October 2000. Additional continuous observation in the northwest mountainside of Mt. Fuji had also been started by utilizing electrical power and communication line of Remote GNSS Monitoring System (REGMOS) at Fuji Oniwa. Furthermore, Earthquake Research Institute, the University of Tokyo has conducted continuous total geomagnetic field observation at Fuji Yoshida (FJ1) and continuous geomagnetic observation at Yatsugatake (YAT). These data are also available and useful to monitor and understand geomagnetic variation around the Mt. Fuji.

Although GSI has been monitoring total geomagnetic field difference between the station at the bottom, FJI, and the stations at the mountainside, FUJ and REGMOS, it is almost impossible to identify variation truly caused by volcanic activities because total geomagnetic field around volcanoes can be fluctuated by both volcanic activities and locally unique geomagnetic variation as well as earth's main magnetic field and external magnetic field variation. Therefore, GSI tries to extract volcano-induced total geomagnetic field variation from the observation data around Mt. Fuji by principal component analysis, and develop monitoring strategy by principal component analysis of total geomagnetic fields around Mt. Fuji.

Keywords: Total geomagnetic field, Mt.Fuji, principal component analysis

## Classification of tsunami dynamo phenomena in terms of ocean depths

MINAMI, Takuto<sup>1\*</sup> ; TOH, Hiroaki<sup>1</sup>

<sup>1</sup>Graduate School of Science, Kyoto University

Conductive seawater moving in the geomagnetic main field drives an electromotive force and induces secondary electromagnetic (EM) fields. This effect is well known as "oceanic dynamo effect" and has been investigated for many years, especially for low-frequency phenomena such as tides and steady oceanic flows. However, it was recently found that tsunamis are also significant sources of the oceanic dynamo effect. Toh et al. (2011) reported tsunami-induced EM field data observed at the northwest Pacific seafloor EM station (NWP) at the time of the 2006/2007 Krill tsunamigenic earthquakes. Ever since, many events associated with the oceanic dynamo effect by tsunamis, hereafter called "tsunami dynamo effect", have been reported (e.g., Manoj et al. 2011; Suetsugu et al., 2012; Ichihara et al., 2013). To explain the tsunami dynamo effect, most of the preceding studies adopted analytical approaches in the frequency domain (e.g., Tyler, 2005). However, it is difficult to understand how EM fields are generated by tsunami propagations, although analytical solutions are very useful and handy.

In order to understand the tsunami dynamo effect more physically, we compared analytical solutions and results of numerical simulations using solitary waves, and revealed that tsunami dynamo phenomena can be classified according to the influence of the diffusion term in the induction equation for the magnetic field. In tsunami dynamo phenomena, the ocean depth has a dominant influence on the diffusion term. When the ocean depth is shallow enough, the diffusion term is large and comparable with the source term, while the self-induction term is small. In this case, the self-induction effect cannot attenuate the magnetic field induced by the coupling of the oceanic flows ( $v$ ) and the geomagnetic main field ( $F$ ), namely  $v \times F$ . We can understand this case mostly by the Ampere's Law. On the other hand, when the ocean depth becomes deeper, the self-induction effect gets larger and reduces the amplitude and causes delay in phase of the magnetic field induced by  $v \times F$ . Especially for the ocean depth deeper than 5000 m, the amplitude is attenuated to approximately 70 percent and the phase is delayed by more than 70 degrees compared with the magnetic field due to  $v \times F$ , which can be understood by analogy with "Frozen Flux". As for the case of the tsunami dynamo phenomena reported by Toh et al. (2011) as well as Minami and Toh (2013), we can regard the phenomena as the self-induction dominant case because the ocean depth at the observation site, NWP, is approximately 5600m. This is consistent with the fact that sea level changes observed at the two DART sites in the vicinity of NWP are in phase with that of the vertical component of the magnetic field observed at NWP. In addition, our analysis using analytical solutions revealed that magnitudes of the tsunami-induced magnetic field have maximum peaks around the ocean depth of 2000m, when the tsunami height is fixed to 1m. This is because the self-induction and the diffusion effect, which vary differently according to the ocean depth, balances around that specific depth. These results are important because they enable us to predict how EM fields are induced by tsunamis in a variety of ocean depths, even though the number of observed examples of tsunami dynamo phenomena is limited at present. It is possible that our results are applied to tsunami early warning or mitigation of tsunami hazards in the future.

In the presentation, we will report the methodology of our classification of tsunami dynamo phenomena and discuss how tsunami-induced EM fields vary according to the ocean depth. We will also discuss how the ocean depth influences on the recently found initial rise (Minami and Toh, 2013) in the horizontal magnetic component observed prior to tsunami arrivals.

Keywords: tsunami, dynamo, solitary wave, seafloor observation, finite element method

## Electric conductivity of earth's medium derived from earthquake-excited electromagnetic signals

TSUTSUI, Minoru<sup>1\*</sup>

<sup>1</sup>Kyoto Sangyo University

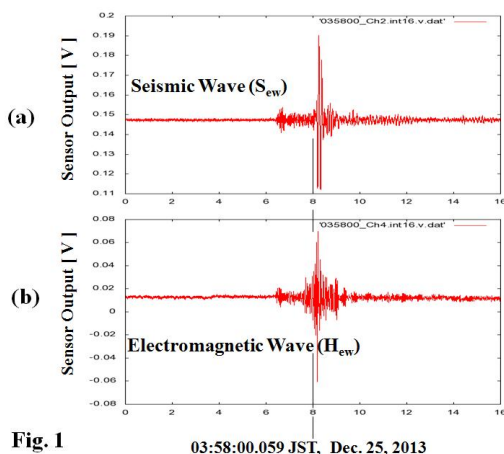
We have been observing electromagnetic (EM) pluses excited by earthquakes, using tri-axial electromagnetic sensors installed in a deep borehole of 100 m in depth. We simultaneously captured waveforms of EM pulses in the borehole and of seismic waves installed near the borehole. We have confirmed that the detected EM waves were co-seismic ones readily generated by piezo-electric effect in earth's crusts [1].

We detected an EM pulse in the borehole when an earthquake of M3.0 occurred at 10 km depth and at 5.4 km north of the EM observation site at 03:57 on Dec. 25, 2013. Figure 1 shows waveforms of (a) east-west component ( $S_{ew}$ ) of the seismic wave, and of (b) east-west component ( $H_{ew}$ ) of magnetic field of the EM pulse. The waveform of the  $S_{ew}$  wave shows an impulsive amplitude at the arrival of its S-wave, which is because the earthquake hypocenter was close to the EM observation site. On the other hand, the waveform of  $H_{ew}$  shows that its amplitude was increasing from about 1 sec prior to the S-wave arrival, and after that it was decreasing.

The amplitude change of  $H_{ew}$  can be explained as follows: Since the electronic conductivity of the earth's medium is large, the amplitude of an EM wave shows an exponential decrease as a function of the distance, in which the decay rate is so-called Skin depth. Since the source of EM pulse was propagating with the S-wave velocity, the amplitude of the EM wave measured at the EM observation site is exponentially increasing as time goes on, and after the S-wave arrival it is exponentially decreasing. Therefore we obtained the Skin depth  $\delta$  for the frequency of 20 Hz and the electronic conductivity as 850 m and 0.0175 S/m, respectively.

[1] M. Tsutsui, submitted to IEEE Geoscience, Letters, 2014.

Keywords: seismic wave, electromagnetic wave, observation in the earth, skin depth, electric conductivity



## Electrical conductivity structures of volcanic areas: a proxy for volcanic gas fluxes

KOMORI, Shogo<sup>1\*</sup>; KAGIYAMA, Tsuneomi<sup>2</sup>; FAIRELY, Jerry<sup>3</sup>

<sup>1</sup>Institute for Earth Sciences, Academia Sinica (Taiwan), <sup>2</sup>Aso Volcanological Laboratory, Kyoto University, <sup>3</sup>University of Idaho

The efficiency of degassing of volcanic gases in magma is one of the key parameters controlling the explosive potentiality of the eruption and the diversity of the volcanic activity. Therefore, to evaluate the mass flux of volcanic gases is important in considering the constraint conditions of the activity. When volcanic gases are dissolved into the pore water of an aquifer, the aquifer has a high electrical conductivity (E.C.); this is because that the pore water conductivity is increased due to the high-salinity and temperature, and that the surface conductivity of rock matrices is also increased due to hydrothermal alteration. Therefore, the spatial extent of the high E.C. region could be related to the abundance of the mass flux of volcanic gases. We have developed the method to estimate the mass flux of volcanic gases using the E.C. structure of volcanic areas as follows.

[Effect of exposure temperatures on the surface conductivity of rock matrices]

There has already been some quantitative formula about the effect of temperature and salinity on the E.C. of the pore water. On the other hand, it has been known that temperatures are closely related to the generation/stability of smectite, which makes a great contribution to the increase of E.C. However, their effect on the surface conductivity has not been understood quantitatively. We performed the E.C. measurements using drillcore samples obtained from drilling projects, to estimate the surface conductivity. Results showed that the relation between surface conductivities and the temperatures to which the rock matrices have been exposed well corresponds to generation/stable condition of smectite. Thus, the surface conductivity could be represented as relatively simple function of exposure temperatures, and the formula could be incorporated into the modeling of dissipation of volcanic gases (Komori et al., 2010, 2013).

[Simplified model for the dissipation of volcanic gases and its application to Unzen volcanic area]

In Unzen volcanic area, there are various geophysical and geochemical studies to understand the formation process of hot springs associated with magma degassing and the magmatic activity. Ohba et al. (2008) proposed three-stage magma degassing; the first magma degassing occurs at the depths of 4-6 km. Correspondingly, the pressure sources are estimated at the similar depths (Kohno et al., 2008). In addition, the high temperature region greater than 200 °C are present above the sources (NEDO, 1988), which corresponds to the high E.C. region inferred from TDEM surveys (Srigutomo et al., 2008).

Based on the above background, we developed the simple model of volcanic gases dissipation into the aquifer at the area, to estimate the mass flux of volcanic gases. The model assumes the isotopic physical properties and the simple geometry of the aquifer. The temperatures and salinity of the pore water are distributed by the simulated flow regime, which is the consequent of the injection of the thermal waters formed by the mixing between volcanic gases and groundwater. Their distributions are converted to the pore water and surface conductivities; which are then converted to the bulk E.C. Results showed that the spatial extent of the high E.C. region is essentially controlled by the volcanic gases flux and rainfall recharge (Komori et al., under review).

[Possibility of effective magma degassing]

The above model was applied to the E.C. structure of the area. The estimated volcanic gas flux was  $10^{4.8 \pm 0.5}$  t/yr, yielding the CO<sub>2</sub> flux ( $10^{3.1 \pm 0.5}$  t/yr) and the magma input rate ( $10^{0.1 \pm 0.5}$  million t/yr). These values are consistent with other petrology, geochemical and geophysical evidences. Our result suggests that the magma is steadily releasing the volcanic fluids into the aquifer. This effective degassing might lead to the decrease of water content of magma, and be one of the reason of the recent effusive volcanism like dome-forming eruptions (Komori et al., under review).

Keywords: Bulk electrical conductivity, Pore water conductivity, Surface conductivity, Volcanic gas fluxes, Unzen volcanic area

## Audio frequency magnetotelluric imaging and tectonic activity evaluation of the Cimandiri Fault, West Java, Indonesia

FEBRIANI, Febty<sup>1\*</sup> ; YAMAYA, Yusuke<sup>2</sup> ; HATTORI, Katsumi<sup>1</sup> ; WIDARTO, Djedi S.<sup>3</sup> ; HAN, Peng<sup>1</sup> ; YOSHINO, Chie<sup>1</sup> ; NURDIYANTO, Boko<sup>4</sup> ; EFFENDI, Noor<sup>4</sup> ; MAULANA, Iwan<sup>4</sup> ; GAFFAR, Eddy<sup>5</sup>

<sup>1</sup>Chiba University, <sup>2</sup>National Institute of Advanced Industrial Science and Technology, <sup>3</sup>Upstream Technology Center, <sup>4</sup>Indonesian Geophysical, Meteorological, Climatological Agency (BMKG), <sup>5</sup>Research Center for Geotechnology, Indonesian Institute of Sciences (LIPI)

The tectonic activity around the Cimandiri fault zone, Pelabuhan Ratu, West Java, Indonesia, has been analyzed for 30 years (1973-2013). The subsurface electrical resistivity structure close to the Cimandiri fault has been also investigated by twenty five audio-magnetotelluric (AMT) sites. The AMT exploration was carried out during two weeks, from July 27, 2009 to August 8, 2009. The sites were distributed on two lines along about 13 km x 6.5 km profile. There are two profiles of the AMT: (1) the A-A' line of the AMT which is perpendicular to the fault (2) the B-B' line of the AMT which is parallel to the fault. Two-dimensional modelling using the code developed by Ogawa and Uchida 2-D inversion has been applied in the AMT data. The result of tectonic activity analysis shows that the Cimandiri fault is the active fault. The subsurface electrical resistivity structure of the Cimandiri fault zone is characterized by (1) the A-A' and B-B' lines present a conductive zone (1-100  $\Omega$ m) from the surface up to the depth of 1 km, which is possibly associated with quaternary volcanics. At the surface, there are also some very conductive spots (1-5  $\Omega$ m) which are indicating the existence of the marine sediments in the study area. (2) The gradual conductive-resistive (500-1,000  $\Omega$ m) zone at the depth of 1-3.5 km overlays above a low resistivity zone (10-100  $\Omega$ m). This low resistivity zone may reflect the combined influences of a fluid network and the presence of the young and less compact sediments with the 500-1,000  $\Omega$ m zone as a cap rock that defines the upper boundary of the low resistivity zone (10-100  $\Omega$ m). Finally, the result of both methods presents that the Cimandiri fault is the strike-slip fault.

Keywords: audio frequency magnetotelluric, subsurface electrical resistivity structure, 2-D inversion, Cimandiri Fault, Indonesia

## Robust magnetotelluric inversion

MATSUNO, Tetsuo<sup>1\*</sup> ; CHAVE, Alan<sup>2</sup> ; JONES, Alan<sup>3</sup> ; MULLER, Mark<sup>3</sup> ; EVANS, Rob<sup>2</sup>

<sup>1</sup>National Institute of Polar Research, <sup>2</sup>Woods Hole Oceanographic Institution, <sup>3</sup>Dublin Institute for Advanced Studies

A robust magnetotelluric (MT) inversion algorithm has been developed on the basis of quantile-quantile (q-q) plotting with confidence band and statistical modelling of inversion residuals for the MT response function (apparent resistivity and phase). Once outliers in the inversion residuals are detected in the q-q plot with the confidence band and the statistical modelling with the Akaike information criterion, they are excluded from the inversion data set and a subsequent inversion is implemented with the culled data set. The exclusion of outliers and the subsequent inversion is repeated until the q-q plot is substantially linear within the confidence band, outliers predicted by the statistical modelling are unchanged from the prior inversion, and the misfit statistic is unchanged at a target level. The robust inversion algorithm was applied to synthetic data generated from a simple 2-D model and observational data from a 2-D transect in southern Africa. Outliers in the synthetic data, which come from extreme values added to the synthetic responses, produced spurious features in inversion models, but were detected by the robust algorithm and excluded to retrieve the true model. An application of the robust inversion algorithm to the field data demonstrates that the method is useful for data clean-up of outliers, which could include model as well as data inconsistency (for example, inability to fit a 2-D model to a 3-D data set), during inversion and for objectively obtaining a robust and optimal model. The present statistical method is available irrespective of the dimensionality of target structures (hence 2-D and 3-D structures) and of isotropy or anisotropy, and can operate as an external process to any inversion algorithm without modifications to the inversion program.

Keywords: Inversion, Probability distribution, Magnetotellurics



## Preliminary report of self-potential observation during a water injection experiment at 1800 m depth in Nojima fault

MURAKAMI, Hideki<sup>1\*</sup> ; HIGA, Tetsuya<sup>2</sup> ; SUZUKI, Takeshi<sup>2</sup> ; YOSHIMURA, Ryokei<sup>2</sup> ; GOTO, Tada-nori<sup>3</sup> ; KAWASAKI, Shingo<sup>4</sup> ; OUCHI, Yuhei<sup>5</sup> ; YAMAGUCHI, Satoru<sup>6</sup>

<sup>1</sup>Natural Sciences Cluster-Science Unit,Research and Education Faculty,Kochi University, <sup>2</sup>Graduate School of Science,Kyoto University, <sup>3</sup>Graduate School of Engineering,Kyoto University, <sup>4</sup>Disaster Prevention Research,Kyoto University, <sup>5</sup>Faculty of Science, Osaka City University, <sup>6</sup>Graduate School of Science,Osaka City University

We report self-potential variations during 2013 water injection experiment at 1800 depth in Nojima fault, which is a surface earthquake fault of the 1995 Hyogoken-nanbu earthquake (Mw6.9). The 2013 water injection test started in 15 September and ended in 29 September. Fresh water was injected into the fault system through the open hole part of the borehole (1800m depth). Average injection rate was 20 liter/min and pressure was 5 MPa. Self-potential variations around the 1800m borehole were very smaller than those in the previous water injection experiments (1997, 2000, 2003, 2004, 2006, and 2008) at 540m depth and self-potential variations did not appear clearly to correspond to the operation of the water injection. The previous water injection experiments have been repeated in the same conditions. The observed variations during the experiments have the following features: 1) self-potential variations appeared to correspond to the operation of water injections; 2) the negative voltage appeared around the water injection borehole, and 3) the magnitude of self-potential variations decreased with increasing distance from the borehole. And the self-potential variations in the previous experiments have become larger every experiment. These features suggest that the observed variations were caused by the streaming potential and the permeability around the open hole part of the borehole (540m depth) has decreased. If the line source model to explain the self-potential variations associated with the water injection is correct, the small self-potential variations observed this experiment may suggest that the permeability of the fault fracture zone at 1800m depth is larger than that around the fault at 540m depth.

Keywords: Nojima fault, 1995 Hyogoken-nanbu earthquake, self-potential, water injection experiment, streaming potential